Diffusion and Disappearance of Traffic Congestion under Steady State in a Graph Network

Masaru Kaji[1,2]

[1]*Graduate School of Decision Science and Technology, Tokyo Institute of Technology,*
2-12-1 Ookayama, Meguro-ku, Tokyo 152-8552, Japan
[2]*Japan Society for the Promotion of Science,*
8 Ichibancho, Kojimachi, Chiyoda-ku, Tokyo, 102-8472, Japan

Keywords: Traffic Jam, Wave Propagation, Alleviation of Congestion, Steady State, Graph Theory.

Abstract: Traffic jams on highways or crowds of people in stations during rush hours are social phenomena that have attracted the attention of many scientists. It is known that the *stop-and-go wave* is a cluster wave that propagates in a direction opposite to the movement of vehicles or pedestrians. A city consists of many roads and intersections in the form of a network, and the stop-and-go wave will propagate according to the road network. Therefore, observations need to be made from a broader perspective to analyze the interconnections between roads when considering traffic congestion. In this study, we use a graph-based control method and define a graph-shaped traffic network considering the characteristics of traffic flow. We set the steady state as the initial condition in the network and create a traffic jam on a certain road intentionally. Following the congestion, we show the manner in which the traffic congestion wave spreads, and discuss the mechanism in which it propagates from one road to a connecting road. This also shows the kind of situations in which traffic jams propagate and diminish; the simulation results correspond to the theoretical value integrated quantitatively. This will be helpful in solving the traffic congestion problem.

1 INTRODUCTION

Traffic jams in urban areas have been a major problem for a very long time. We can primarily observe this phenomenon in stations during rush hours (pedestrian dynamics) or on highways (vehicular dynamics) on a daily basis. Traffic jams cause inefficient flow of pedestrians or vehicles,and may even lead to a crash involving several vehicles or a pedestrian crowd disaster. To solve this problem, many researchers have studied the characteristics of traffic dynamics. For example, the traffic flow efficiency rapidly decreases when a traffic jam occurs because the traffic density is greater than a threshold value for both pedestrian traffic(Polus et al., 1983; Mori and Tsukaguchi, 1987; Helbing and Al-Abideen, 2007; Kretz and Schreckenberg, 2006) and vehicular traffic (Kerner and Rehborn, 1997; Kerner, 1998; Geloliminis and F., 2008; Daganzo et al., 2011). Moreover, the traffic jam results in a cluster that consists of some vehicles and the cluster moves in a direction opposite to the movement of vehicles on the highway (Kerner and Rehborn, 1997; Kerner, 1998). This phenomenon is also confirmed in pedestrian dynamics (Helbing and

Al-Abideen, 2007; Kretz and Schreckenberg, 2006; Zhang et al., 2012; Jiayue et al., 2014). Pedestrians or vehicles that are involved in the congestion reduce their speed and stop. They start to move again when the vehicle or the pedestrian ahead moves. On the basis of the series of these movements, scientists call this wave propagation a *stop-and-go wave*.

Thus far, most studies on traffic flow have considered only one subsystem such as a road (Polus et al., 1983; Mori and Tsukaguchi, 1987; Kerner and Rehborn, 1997; Kerner, 1998; Geloliminis and F., 2008; Daganzo et al., 2011; Zhang et al., 2012), an intersection (Lammer and Helbing, 2008; Papageorgiou et al., 2003), or a junction (Kerner and Rehborn, 1997; Kerner, 1998; Papageorgiou et al., 2003). However, in real-time traffic, paths for pedestrian movement and roads for vehicles are connected and extend in a network through intersections or junctions. The effect of the traffic condition on a road is transmitted to the adjacent roads via the joint. Therefore, we need to discuss the macroscopic system as a composite subsystem. In fact, recently, traffic dynamics has been studied in terms of a complex network (Geloliminis and F., 2008; Daganzo et al., 2011; Lammer and Helbing,

2008; Shen and Gao, 2008; Ezaki et al., 2015; Kaji, 2016; Tao et al., 2016; Sun et al., 2015; Papageorgiou et al., 2003). Shen and Gao (Shen and Gao, 2008) analyzed the relationship between the dynamical properties of transportation and the structure network on a scale-free network. Geloliminis et al. (Geloliminis and F., 2008) presented a macroscopic fundamental diagram (MFD) at a city-scale level in Yokohama, Japan. They suggested that the MFD relating the average vehicle density and space-mean vehicle flow in the city exists for the complete network. Ezaki et al. (Ezaki et al., 2015) assumed a traffic network and developed a transportation control method considering traffic characteristics such as those in (Polus et al., 1983; Mori and Tsukaguchi, 1987; Helbing and Al-Abideen, 2007; Kretz and Schreckenberg, 2006; Kerner and Rehborn, 1997; Kerner, 1998; Geloliminis and F., 2008; Daganzo et al., 2011). They also calculated the transition boundary condition of the breakdown of the system in the network, and showed that the theoretical value matched the simulation result on a certain region. Tao et al. (Tao et al., 2016) studied the influence of congestion propagation in a traffic network by using the Cell Transmission Model (CTM) theory. They then confirmed the congestion affects both the upstream and downstream regions of the road through joints such as the intersection.

In this paper, in contrast to (Tao et al., 2016), we study the effect of a wave cluster of the traffic jam in a road network more qualitatively and quantitatively, by using the model of (Ezaki et al., 2015). The cluster wave will affect another road and we can predict that the traffic jam propagates to the other adjacent roads and then finally diminishes. In this case, a new crucial consideration is analyzing how the traffic jam spreads and in what kind of situations traffic congestion vanishes. It is important to consider the effect of a stop-and-go wave in a road network for the prediction of a dynamical traffic jam. Therefore, we study the dynamics by considering graph theory and an improved control simulation method of closing and opening of inflow (Ezaki et al., 2015). We assume a traffic road network considering traffic characteristics such as the free-flow state and the jammed state. Moreover, we set the steady state as the initial condition and create a traffic jam by closing a certain road intentionally. Consequently, we analyze the effect of traffic congestion, discuss diffusion and alleviation of the traffic jam, and discuss qualitatively the conditions under which the traffic congestion vanishes in the model.

This paper is organized as follows. Section 2 describes the graph used in this study and the simulation method. In Section 3, we show the results of this simulation and interpret them to qualitatively explain how the traffic jam spreads and quantitatively determine the situations in which traffic congestion vanishes in the graph. Finally, we state the conclusions and areas for future research in Section 4.

2 METHOD

To prepare the traffic network, we use graph theory for analyzing the flow state in digraph. Graph G in this study consists of a set V_d of vertices and a set A_d of arcs ($A_d \subset V_d \times V_d$). Note that a vertex and an arc represent a crossing and a one-way street, respectively. Each arc represents a connection from a vertex to another vertex so as to not encounter a dead end. All in-degrees and out-degrees in G have the same value, i.e. three, as shown in Fig. 1a. Therefore, graph G is a cubic directed closed graph. Furthermore, we assume that the number of vertices |G| and arcs ‖G‖ is 200 and 600, respectively. To visualize the state in G clearly, we draw 10 vertices vertically, and 30 vertices horizontally. Each arc is connected from a vertex to the three neighboring vertices on the right, and the rightmost vertices are joined to the three leftmost ones. Thereby, we assume that G is periodic and has a directional structure from left to right. In addition, we connect the uppermost vertices and the lowermost vertices to include the effect of the opposite arc. Therefore, the structure of G is Torus and Fig. 1b is the development elevation of G. Moreover, we regard a_{ij} as an arc connecting vertex i to vertex j ($i \neq j \mid i, j \in V_d$). Every arc includes any number of objects and the density of the objects in a_{ij} at time step t is $\rho_{ij}(t)$. We define the outflow from a_{ij} as F_{out} (ρ_{ij}) ($0 \leq \rho, F_{out} \leq 1$). The transportation efficiency is rapidly decreased and a traffic jam occurs when the pedestrian or vehicle density is over a critical density. Based on the traffic characteristics, we determine the value of F_{out} as follows:

$$F_{out}(\rho) = \min\left\{ \frac{\rho}{2\rho^*}, \frac{1-\rho}{2(1-\rho^*)} \right\}. \qquad (1)$$

This simple function expresses the free-flow state and the jammed state (Fig. 1c). In general, vehicles or pedestrians can move smoothly in the free-flow state. In the jammed state, on the other hand, the traffic flow becomes inefficient and there is a possibility that traffic congestion might occur. Note that Ezaki et al. (Ezaki et al., 2015) assumed that every vertex included some density instead of every arc and discussed the interaction between each vertex; however, we assume that there is some density in each arc to consider a more realistic situation in the scenario when vehicles or pedestrians move in the network.

When the density in an arc is greater than the threshold ρ_{cl}, we prevent inflow into the arc by closing the entrance of the arc, allowing only outflow from the arc. Furthermore, a closed arc is opened when the density of the arc is less than ρ_{op} by discharging the density into another arc. With regards to the inflow rule, we consider a detouring pattern. In the detouring pattern, the objects flowing from the departure arc are distributed equally in all open arcs. If all three destination arcs are closed, the outflow from the arc is canceled. In addition, the time development of density on arc a_{ij} at t is given by

$$
\begin{aligned}
\frac{d\rho_{ij}(t)}{dt} &= Q_{in}(a_{ij},t) - Q_{out}(a_{ij},t) \\
&= \frac{1}{3}\sum_{h}^{V_d} A_{hi}B_{ij}F_{out}(\rho_{hi}(t)) \\
&\quad -\frac{1}{3}\sum_{k}^{V_d} A_{jk}B_{jk}F_{out}(\rho_{ij}(t)), \quad (2)
\end{aligned}
$$

where $Q_{in}(a_{ij},t)$ and $Q_{out}(a_{ij},t)$ are the total inflow to a_{ij} and outflow from a_{ij}, respectively. Note that the transfer flow depends on conditions at the current arc and downstream. Moreover, A_{ij} is 1 when there is an arc from vertex i to vertex j ($i, j \in V_d$, $i \neq j$), otherwise A_{ij} is 0. Furthermore, B_{ij} is 1 or 0 depending on whether a_{ij} is opened or closed, respectively. Apart from the detouring pattern, we can also consider a queuing pattern in which the objects flowing from the departure arc stay there if the arrival arc is closed. However, the queuing pattern has already been studied in (Kaji, 2016). We discuss only the case of the detouring pattern in this study.

We define the vertices and arcs first in our simulation. After that, the initial density at each arc is set as $t = 0$. Then, the density in each arc is calculated according to the above-mentioned rules. After this calculation, the density in each arc is updated. Afterwards, t is updated to (t+dt). The simulation is conducted until $t = 100$. In this study, we conduct simulations with dt = 0.0001. Fig. 2 shows the flowchart in this simulation. We set $\rho_{cl} = 0.75$, and $\rho^* = 0.5$ for simplicity.

In this simulation, we assume that every arc in G is uniformly set with the average density $\overline{\rho}$ by the initial condition, and the amount of inflow is the same as the amount of outflow, i.e., the initial flow in G is in a steady state. Then, we generate a traffic jam in an arc intentionally in graph G at $t = 0$. We set the density in the arc, located on the right center in G in Fig.1b, as ρ_{cl}, and we set the state of the arc as closed. In this way, we can analyze the effect of this on the surrounding arcs.
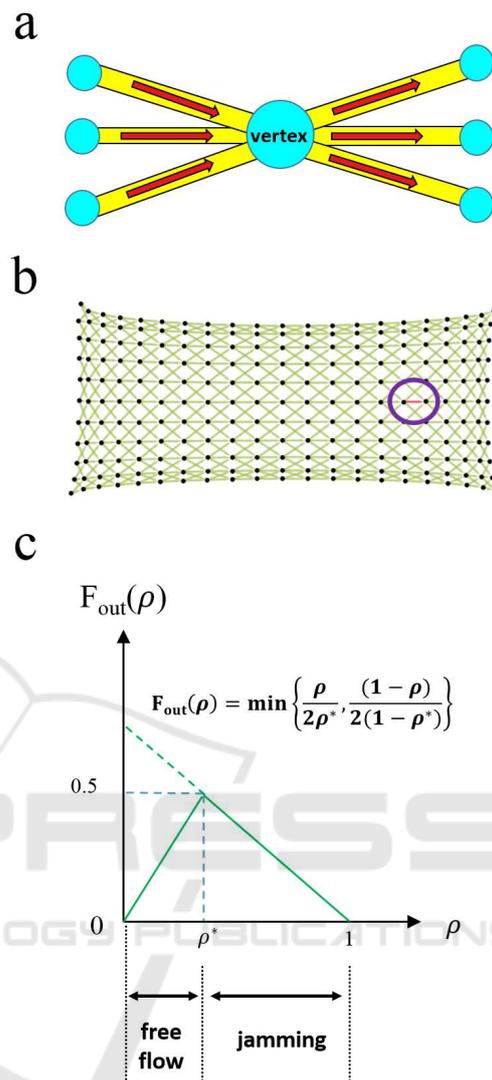
Figure 1: (a) Diagram of a vertex with three arcs connected from and three arcs connected to other vertices. (b) The developed elevation of G. The uppermost vertices are the same as the lowermost vertices. In the same way, the rightmost vertices are the same as the leftmost vertices. Therefore, the structure of G is Torus and the objects move from left to right. In this simulation, we generate a traffic jam intentionally in an arc surrounded by the purple circle (the red arc). (c) Function $F_{out}(\rho)$ versus the density ρ.

3 RESULTS AND DISCUSSION

3.1 State of the Graph after the Occurrence of Traffic Congestion

When viewing the state of G at $t = 100$ and $\rho_{op} = 0.60$, there are roughly three phases, i.e., the free-flow
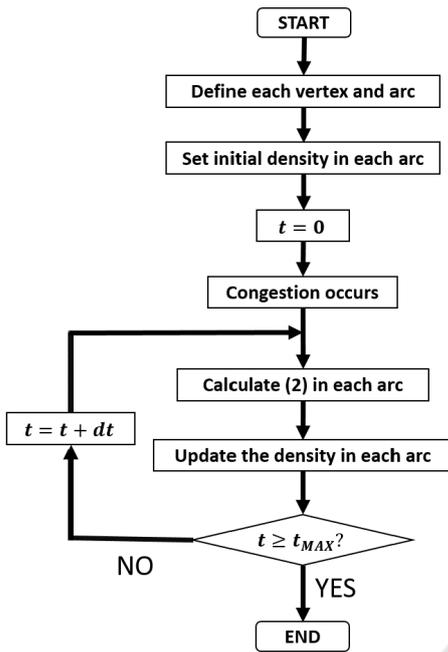
Figure 2: Flowchart used in this study.

Figure 3: States in the graph in the case of the free-flow phase, the controlled phase, and the deadlock phase where $\rho_{op} = 0.60$, at $t = 100$, and (a) $\overline{\rho} = 0.35$, (b) $\overline{\rho} = 0.60$, and (c) $\overline{\rho} = 0.75$. The value of density matches the color bar.

phase, the controlled phase, and the deadlock phase, which are obtained by changing $\overline{\rho}$ (Fig. 3). Note that the red arcs in Fig. 3 express the closed state. In the free-flow state, traffic congestion is solved immediately and the state in G returns to the original steady state (Fig. 3a). In the case of the controlled phase, some congestion continues to exist locally in G and moves from an arc to another arc (Fig. 3b). On the other hand, in the deadlock phase, all arcs in G are closed and the flow in G breaks down because of the congestion generated at $t = 0$ (Fig. 3c).

We show the phase diagram in the $\overline{\rho}$ and ρ_{op} plane at $t = 100$ in Fig. 4a. From this figure, we can see that the phase depends on $\overline{\rho}$ and ρ_{op}. The area $*$ in Fig. 4a is a kind of controlled phase. In this area, only the arc in which congestion was generated intentionally repeats the steps of closed and opened states as ρ_{op} is relatively large and the flow is always inefficient even if the arc is opened. Furthermore, we calculated the average flow rate in G. We defined the average flow rate as $\overline{Q} = \frac{\sum_i^{V_d} \sum_j^{V_d} A_{ij} Q_{out}(a_{ij})}{\|G\|}$. The MFD is shown in Fig. 4b. Figs. 4a and 4b show that efficient flow is achieved in the free-flow state, and also show the average flow rate $\overline{Q}$ in the graph along with the value of function (1) when $\rho^* = \frac{1}{2}$. Here $\overline{Q}$ rapidly decreases just as the phase changes from the free-flow phase to the controlled phase, and is gradually reduced as $\overline{\rho}$ increases. Eventually, $\overline{Q}$ is 0 in the deadlock phase. Note that the flow rate in $*$ achieves efficient flow because there is only one closed arc.

3.2 How the Traffic Congestion Spreads

We analyzed the controlled phase in detail. In this phase, we can divide the movement of the congestion into four patterns by changing the parameters ρ_{op} and $\overline{\rho}$. Fig. 5 shows a snapshot for each of these simulations. In Fig. 5a, the congestion in the arc propagates in a direction opposite to the movement of objects (to the left) as a recession wave and crosswise (to the vertical). The width of the wave gradually increases and the wave transforms into a large one. In Fig. 5b, the movement of the wave is the same as that of the wave in Fig. 5a in the early stage. However, the rear part of the congestion wave (right side) is stagnant in some arcs. The speed of the nose of the wave gradually decreases. In Fig. 5c, the congestion arc affects not only the direction opposite to the movement of the objects, but also the direction of the movement of the objects (the traveling wave). After a while, the traveling wave collides with the recession wave, forms some new waves, and moves to the left in the graph. In Fig. 5d, on the other hand, the movement of the wave exhibits the same behavior as that in Fig. 5c in an early stage. After that, the congestion wave does not grow and each congestion wave continues to move finely in the graph. In general, we confirmed the phenomenon in Figs 5a and 5b when $\overline{\rho}$ is less than 0.5 (more generally speaking, $\overline{\rho} \leq \rho^*$).

189
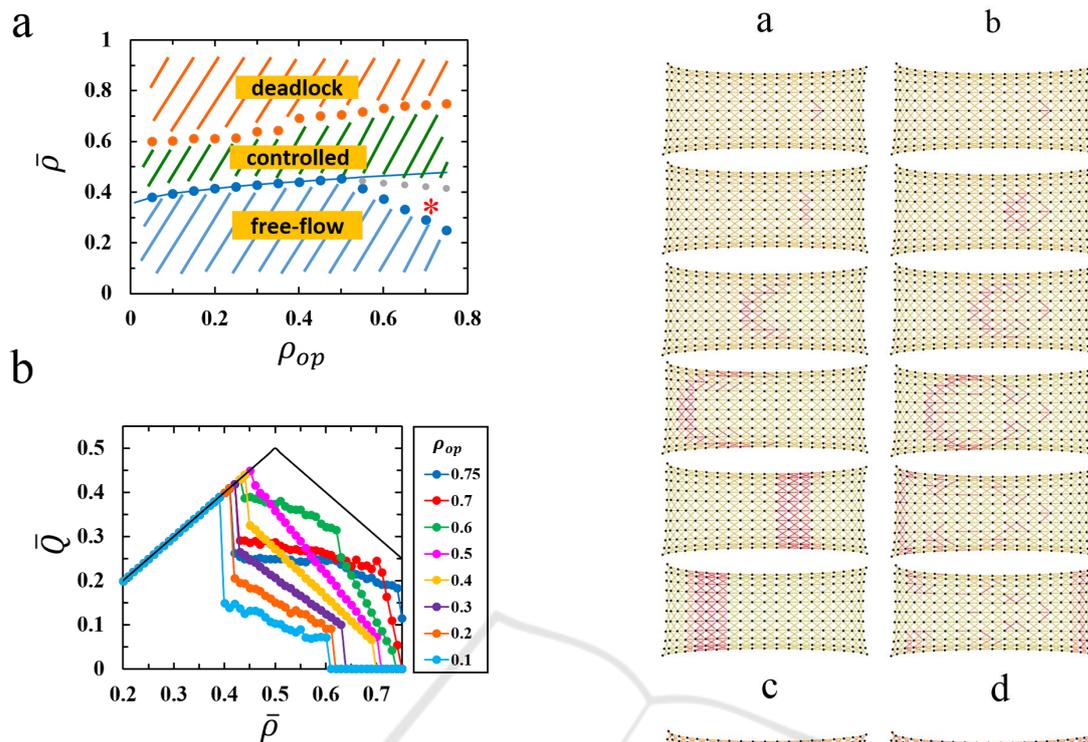
Figure 4: (a) Phase diagram for this simulation. The vertical and the horizontal axes represent the open arc density ρ_{op} and the average density $\overline{\rho}$, respectively, at $t = 100$ and $\rho^* = 0.5$. The blue circles indicate the border between the free-flow phase and the controlled phase. The orange circles indicate the border between the controlled phase and the deadlock phase. The area within the star surrounding the blue circles and the gray circles show the phase in which the only arc where congestion was generated intentionally repeats the steps from being in the closed state to the open state and vice versa. The blue solid line is the theoretical value of the function (7). (b) Macroscopic fundamental diagram of Fig. 4a. The vertical and the horizontal axes denote the initial average density $\overline{\rho}$ and the average flow rate $\overline{Q}$, respectively. The solid line corresponds to function (1).

Otherwise, the phenomenon shown in Figs. 5c and 5d occurs. Moreover, the simulation result shown in Fig. 5a is found to hold when ρ_{op} is relatively small. The result gradually has the nature of Fig. 5b from when ρ_{op} is approximately 0.55. On the other hand, the phenomenon in Fig. 5c begins to move into that of Fig. 5d when ρ_{op} is about 0.58. Both the recession wave and the traveling wave propagate faster as the initial average density increases.

Next, we discuss the mechanisms of the phenomenon in which the congestion wave moves in a direction opposite to the movement of objects as observed in Figs. 5a, 5b, 5c, and 5d. When traffic congestion occurs in an arc, the outflow from the three arcs located on the next congestion arc to the right is
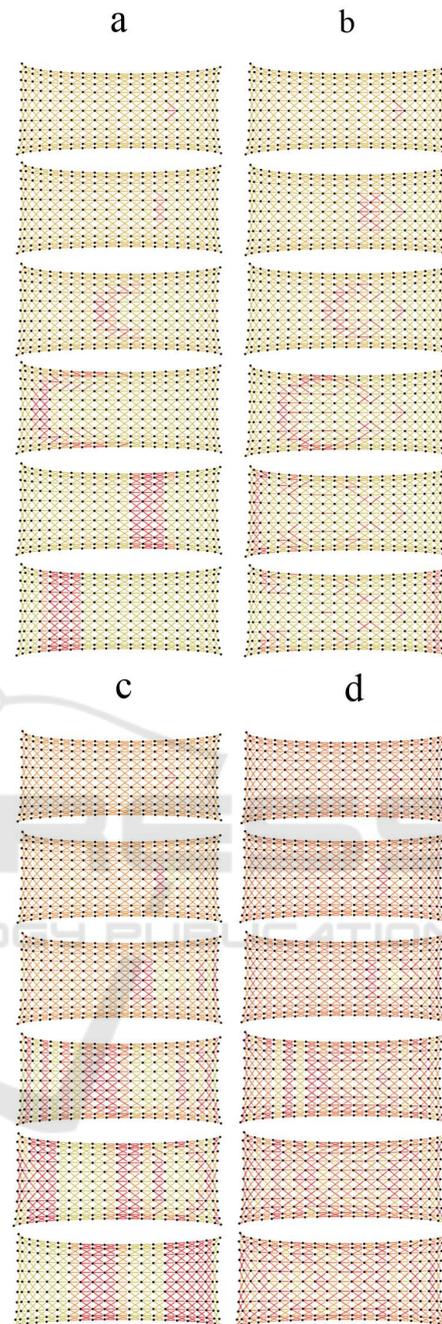
Figure 5: Snapshots of the wave propagation by the four patterns in the controlled phase. The conditions are: (a) ρ_{op} = 0.40, $\overline{\rho}$ = 0.45, at t = 3, 5, 10, 15, 25, and 45; (b) ρ_{op} = 0.60, $\overline{\rho}$ = 0.45, at t = 9, 15, 20, 30, 40, and 50; (c) ρ_{op} = 0.40, $\overline{\rho}$ = 0.55, at t = 1, 2, 3, 5, 10, and 20; and (d) ρ_{op} = 0.60, $\overline{\rho}$ = 0.60, at t = 1, 2, 3, 5, 10, and 20.

limited. Despite this, the inflow to these three arcs does not change. Hence, the density of these arcs gradually increases. As a result, these three arcs fall into a state of congestion. This event successively

propagates in a direction opposite to the movement of the recession wave.

In the case of the phenomenon in which the rear part of the congestion wave (right side) is stagnant in some arcs in Figs 5b and 5d, the congestion arc cannot recover from the jammed state to the free-flow state easily because the value of ρ_{op} is relatively large and the flow soon becomes inefficient, even if the arc returns from the closed state to the open state. Thereby, the arc is no longer in the inefficient flow state and alternates between the closed and the open states.

When the traveling wave occurs as shown in Figs 5c and 5d, the outflow from the congestion arc is relatively small compared with the outflow from the three arcs, which are located on the right side of the congestion arc. Therefore, the density in these arcs gradually decreases, and the outflow from these arcs increases. Thereby, the inflow of the following arcs on the right increases and so does the density of these arcs. Finally, these arcs transit from the inefficient flow state to the congestion state. By repeating the mechanism in a direction to the right, the wave propagates to the right. This phenomenon occurs when $\overline{\rho} > \frac{1}{2}$ (speaking more generally, $\overline{\rho} > \rho^*$). However, the phenomenon will not occur intuitively in a real-time vehicle or pedestrian dynamics because the traffic congestion affects the vehicles or pedestrians at the rear when the general stop-and-go wave propagates backward.

3.3 Kinds of Situations in which the Traffic Congestion Vanishes

We now discuss the phase transition to determine whether a congestion arc affects the arcs at the back (to the left in this simulation) or not. In this paper, we discuss only $\rho_{op} \leq \frac{1}{2}$ (or $\rho_{op} \leq \rho^*$). When an arc is congested with traffic (the closed state), we need to consider the critical density ρ', which is the density of the arcs next to the congestion arc on the right when the congestion arc recovers from the closed state to the open state. That is, the congestion arc affects the following arcs if the time $T_{\overline{\rho} \to \rho'}$, which is required for increasing the density of the arcs from $\overline{\rho}$ to the critical density ρ', is greater than the time $T_{\rho_{cl} \to \rho_{op}}$ required for recovering from the closed state to the open state. We can change equation (2) as $dt = \frac{d\rho}{\Delta Q}$, i.e., the normalization constant, $T_{\rho_{cl} \to \rho_{op}}$ can be presented as

$$
\begin{aligned}
T_{\rho_{cl} \to \rho_{op}} &= \int_{\rho_{cl}}^{\rho_{op}} \frac{d\rho}{-Q_{out}} \\
&= \int_{\rho_{op}}^{\frac{1}{2}} \frac{d\rho}{\rho} + \int_{\frac{1}{2}}^{\rho_{cl}} \frac{d\rho}{1-\rho} \\
&= \log \frac{1}{4(1-\rho_{cl})\rho_{op}}.
\end{aligned} \tag{3}
$$

Roughly speaking, the congestion cluster does not propagate unless the inflow in an arc is greater than the outflow on the road. Therefore, when $T_{\rho_{cl} \to \rho_{op}} = T_{\overline{\rho} \to \rho'}$, the boundary condition for whether a congested road affects the adjacent rear roads or not, can be presented as

$$
\rho' = 1 - \overline{\rho}. \tag{4}
$$

Here, we assume that the relation $\overline{\rho} < \frac{1}{2}$ always holds. Intuitively, it is true because of the simulation results in Fig. 4a. Next, from (2), assuming the arc is in the steady state, the time development of the density on an arc, which is located on the congestion arc at the back, becomes

$$
\begin{aligned}
\frac{d\rho}{dt} &= Q_{in} - Q_{out} \\
&= \overline{\rho} - \frac{2}{3} \min\{\rho, 1-\rho\},
\end{aligned} \tag{5}
$$

where Q_{in} is constant $\overline{\rho}$. When $\rho_{op} \leq \frac{1}{2}$, $T_{\overline{\rho} \to \rho'}$ is given by

$$
\begin{aligned}
T_{\overline{\rho} \to \rho'} &= \int_{\overline{\rho}}^{\rho'} \frac{d\rho}{Q_{in} - Q_{out}} \\
&= \int_{\overline{\rho}}^{\frac{1}{2}} \frac{d\rho}{\overline{\rho} - \frac{2}{3}\rho} + \int_{\frac{1}{2}}^{\rho'} \frac{d\rho}{\overline{\rho} - \frac{2}{3}(1-\rho)} \\
&= 2 \int_{\overline{\rho}}^{\frac{1}{2}} \frac{d\rho}{\overline{\rho} - \frac{2}{3}\rho} \\
&= 3 \log \frac{\overline{\rho}}{3\overline{\rho} - 1},
\end{aligned}
$$

$$
\tag{6}
$$
$$
\tag{7}
$$

where (6) is derived from the symmetry that $\rho' = 1 - \overline{\rho}$ as we regard $\rho = \frac{1}{2}$ as a median Assuming that the boundary density $\overline{\rho}_{trans}$ is the average density $\overline{\rho}$ when $T_{\overline{\rho} \to \rho'} = T_{\rho_{cl} \to \rho_{op}}$, we consider the boundary condition (4) and derive from (3) and (7)

$$\overline{\rho}_{trans} = \frac{\left(\frac{1}{4(1-\rho_{cl})\rho_{op}}\right)^{\frac{1}{3}}}{3\left(\frac{1}{4(1-\rho_{cl})\rho_{op}}\right)^{\frac{1}{3}} - 1}. \quad (8)$$

The theoretical values of (8) match the simulation results shown in Fig. 4a.

Moreover, we further generalize (8). When ρ^* is a variable, i.e., when F_{out} satisfies function (1), we can rewrite (3) as

$$T_{\rho_{cl} \to \rho_{op}} = 2\log\left\{\left(\frac{\rho^*}{\rho_{op}}\right)^{\rho^*}\left(\frac{1-\rho^*}{1-\rho_{cl}}\right)^{(1-\rho^*)}\right\}. \quad (9)$$

Furthermore, we derive the boundary condition from (4)

$$\rho' = 1 - \frac{1-\rho^*}{\rho^*}\overline{\rho}. \quad (10)$$

Assume that the relations $\overline{\rho} < \rho^*$ and $Q_{in} = \frac{\overline{\rho}}{2\rho^*}$ are always practical, we can derive from (5) and (10) when $\rho_{op} < \rho^*$ in the relation

$$\begin{aligned}
T_{\overline{\rho} \to \rho'} &= \int_{\overline{\rho}}^{\rho^*} \frac{d\rho}{\frac{\overline{\rho}}{2\rho^*} - \frac{2}{3}\frac{\rho}{2\rho^*}} + \int_{\rho^*}^{\rho'} \frac{d\rho}{\frac{\overline{\rho}}{2\rho^*} - \frac{2}{3}\frac{1-\rho}{2(1-\rho^*)}} \\
&= 3\log\frac{\overline{\rho}}{3\overline{\rho} - 2\rho^*}. \quad (11)
\end{aligned}$$

With (9) and (11), we finally obtain

$$\overline{\rho}_{trans} = \frac{2\rho^*\left(\frac{\rho^*}{\rho_{op}}\right)^{\frac{2}{3}\rho^*}\left(\frac{1-\rho^*}{1-\rho_{cl}}\right)^{\frac{2}{3}(1-\rho^*)}}{3\left(\frac{\rho^*}{\rho_{op}}\right)^{\frac{2}{3}\rho^*}\left(\frac{1-\rho^*}{1-\rho_{cl}}\right)^{\frac{2}{3}(1-\rho^*)} - 1}. \quad (12)$$

Fig. 6 shows the theoretical values of function (12) and the simulation results in each ρ^* where $\rho_{cl} = 0.75$, and each theoretical value and the value from the simulation matches when $\rho_{op} \leq \rho^*$.

4 CONCLUSIONS AND FUTURE RESEARCH

In this paper, we assumed the traffic network to be a cubic directed closed graph considering the traffic characteristics such as the free-flow state and the jammed state. Moreover, we have defined the control method using the closed and open states of inflow. We have set the steady state as the initial condition and generated a traffic jam by closing a certain arc intentionally at a certain time. As a result,
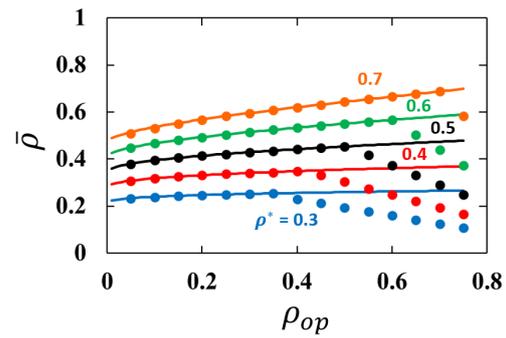
Figure 6: Contour lines between the free-flow phase and the controlled phase where $\rho_{cl} = 0.75$. The solid lines denote the theoretical values of function (8) and the dots denote the simulation results where $\rho_{cl} = 0.75$, ρ^* is 0.3 (blue), 0.4 (red), 0.5 (black), 0.6 (green), and 0.7 (orange). Note that the black dots and line in this figure correspond to the blue dots and the blue line in Fig. 4a.

there arose three traffic phase patterns in the graph, i.e., the free-flow phase, the controlled phase, and the deadlock phase. We have obtained the phase diagram and found that the phase condition depends on the open state density of the arc and the initial average density in the graph. Furthermore, in the controlled phase, we have confirmed that the congestion movement contains three patterns; the recession wave pattern, the traveling wave pattern, and the stagnation pattern, formed by changing the opened density and the initial average density. In addition, we have discussed the quantitative assessment related to the effect of the congestion arc on the other adjacent arcs, i.e., the boundary condition between the free-flow phase and the controlled phase. As a consequence, the theoretical value partially corresponded to the simulation result in the phase diagram. This theory will help us arrive at the solution of the traffic congestion problem.

However, we could not show the theoretical value in certain regions. It is necessary to discuss the remaining portions for more exact prediction. In addition, qualitatively discussing the flow condition in the unsteady state and the inequality distribution rule in a more realistic traffic network remain unsolved challenges. Furthermore, this model will be more realistic model by changing from the deterministic to the stochastic. We also need to confirm whether the simulation and theoretical values match the real-time traffic phenomenon. Finally, by developing the model which can forecast the traffic jam in a road network, we will be able to apply to the operations research model such as the time-dependent shortest path problem in urban network (Cooke and Halsey, 1966; Sun et al., 2017).

ACKNOWLEDGEMENTS

REFERENCES

Cooke, K. and Halsey, E. (1966). The shortest route through a network with time-dependent internodal transit times. 14(3):493–498.

Daganzo, C. F., Gayah, V. V., and Gonzales, E. J. (2011). Macroscopic relations of urban traffic variables: Bifurcations, multivaluedness and instability. *Transportation Research Part B: Methodological*, 45(1):278–288.

Ezaki, T., Nishi, R., and Nishinari, K. (2015). Taming macroscopic jamming in transportation networks. *Journal of Statistical Mechanics: Theory and Experiment*, 2015(6):P06013.

Geloliminis, N. and F., D. C. (2008). Existence of urban-scale macroscopic fundamental diagrams: Some experimental findings. *Transportation Research Part B: Methodological*, 42(9):759–770.

Helbing, D., J. A. and Al-Abideen, H. Z. (2007). Dynamics of crowd disasters: An empirical study. *Physical review E*, 75(4):046109.

Jiayue, W., Wenguo, W., and Xiaole, Z. (2014). Comparison of turbulent pedestrian behaviors between mina and love parade. In *Proceedings of the 2014 International Symposium on Safety Science and Technology*, volume 84, pages 708–714.

Kaji, M. (2016). Analysis of propagation of traffic jam under steady flow (in japanese). In *Proceedings of the 22th Symposium on Traffic Flow and Self-Driven Particles*, pages 65–68.

Kerner, B. S. (1998). Experimental features of self-organization in traffic flow. *Physical Review Letters*, 81(17):3797.

Kerner, B. S. and Rehborn, H. (1997). Experimental properties of phase transitions in traffic flow. *Physical Review Letters*, 79(20):4030.

Kretz, T., G. A. and Schreckenberg, M. (2006). Experimental study of pedestrian flow through a bottleneck. *Journal of Statistical Mechanics: Theory and Experiment*, 2006(10):P10014.

Lammer, S. and Helbing, D. (2008). Self-control of traffic lights and vehicle flows in urban road networks. *Journal of Statistical Mechanics: Theory and Experiment*, 2008(04):P04019.

Mori, M. and Tsukaguchi, H. (1987). A new method for evaluation of level of service in pedestrian facilities. *Transportation Research Part A: General*, 21(3):223–2346.

Papageorgiou, M., Diakaki, C., Dinopoulou, V., Kotsialos, A., and Wang, Y. (2003). Review of road traffic control strategies. In *Proceedings of the IEEE*, volume 91, pages 2043–2067.

Polus, A., Schofer, J., and Ushpiz, A. (1983). Pedestrian flow and level of service. *Journal of Transportation Engineering*, 109(1):46–56.

Shen, B. and Gao, Z. Y. (2008). Dynamical properties of tranportation on complex networks. *Physica A: Statistical Mechanics and is Applications*, 387(5):1352–1360.

Sun, L., Liu, L., Xu, Z., Jie, Y., Wei, D., and Wang, P. (2015). Locating inefficient links in a large-scale transportation network. *Physica A: Statistical Mechanics and is Applications*, 419:537–545.

Sun, Y., Yu, X., Bie, R., and Song, H. (2017). Discovering time-dependent shortest path on traffic graph for drivers towards green driving. *Journal of Network and Computer Applications*, 83:204–212.

Tao, R., Xi, Y., and Li, D. (2016). Simulation analysis on urban traffic congestion propagation based on complex network. In *Proceedings of the IEEE Service Operations and Logistics, and Informatics 2016*, pages 217–222.

Zhang, X. L., Weng, W. G., and Yuan, H. Y. (2012). Empirical study of crowd behavior during a real mass event. *Journal of Statistical Mechanics: Theory and Experiment*, 2012(8):P08012.